Research · Science
Forschung · Wissenschaft
Recherche · Science

Publisher
Herausgeber
Editeur

Schweizerische Zahnärzte-Gesellschaft SSO
Société Suisse d'Odonto-Stomatologie
CH-3000 Bern 7

Editor-in-chief
Chefredaktor
Rédacteur en chef

Prof. Adrian Lussi
Klinik für Zahnerhaltung, Präventiv- und Kinderzahnmedizin
Freiburgstr. 7
3010 Bern

Editors
Redaktoren
Rédacteurs

Andreas Filippi, Basel
Susanne Scherrer, Genève
Patrick R. Schmidlin, Zürich

Assistant Editor
Redaktions-Assistent
Rédacteur assistant

Brigitte Zimmerli, Bern
Klaus Neuhaus, Bern

Jede im Teil «Forschung und Wissenschaft» der SMfZ eingereichte Arbeit wird von zwei bis drei zahnärztlichen Fachpersonen begutachtet. Diese genaue Begutachtung macht es möglich, dass die Publikationen einen hohen wissenschaftlichen Standard aufweisen.

Ich bedanke mich bei den unten aufgeführten Kolleginnen und Kollegen für ihre wertvolle Mitarbeit, die sie in den vergangenen zwei Jahren geleistet haben.

Adrian Lussi

Sandra Luso
Hans Ulrich Luder

Institute of Oral Biology, Center of Dental Medicine, University of Zurich

Correspondence
Prof. Dr. H. U. Luder
Center of Dental Medicine
Institute of Oral Biology
Plattenstrasse 11
8032 Zurich
Tel. 044 634 31 40
Fax 044 634 43 06
E-mail: hansulrich.luder@zzm.uzh.ch

Schweiz Monatsschr Zahnmed 122: 914–922 (2012)

Accepted for publication:
9 February 2012

Resorption pattern and radiographic diagnosis of invasive cervical resorption

A correlative microCT, scanning electron and light microscopic evaluation of a case series

Key words: invasive cervical resorption (external granuloma), X-ray microtomography, microscopic structure, radiographic diagnosis, differential diagnosis

Summary The aim of this study was to evaluate, whether and how the histologic structure of invasive cervical resorption (external granulomas) affect their clinical radiographic diagnosis. For this purpose, nine more or less intact extracted teeth, of which intraoral radiographs were available, were processed for examination in the scanning electron (SEM) and light microscope. From some of the specimens non-decalcified ground sections were prepared and some were decalcified for preparation of histologic sections. Five teeth were scanned in an X-ray microtomography (microCT) device and digitally reconstructed in three dimensions.

Three histologic characteristics, namely (1) the location and extension of the resorptive defect, (2) the size of the communication with the periodontium, and (3) the amount of mineralized substitution tissue formed in the lesion affected the radiographic diagnosis. At early and advanced stages, invasive cervical resorption had encircled the pulp cavities, however, without destroying the innermost dentin. Even if the dentinal wall adjacent to the pulp was histologically intact and thick, this important diagnostic feature frequently could not be recognized in conventional radiographs. Also, the communication between the resorptive lesion and the periodontium often was not visible radiographically, although it could always be identified in the microscopic evaluation, particularly at early stages when it proved to be very small. Invasive cervical resorption lesions containing large amounts of mineralized substitution tissue were difficult to recognize and, therefore, could easily be overseen.

Thus, three features which are deemed essential for the differential diagnosis of invasive cervical resorption were not readily apparent in conventional radiographs. From these three features, the dentinal wall against the pulp cavity and the communication to the periodontium were, however, clearly visible in the microCT reconstructions.

Introduction

Over the past years, the Institute of Oral Biology, Center of Dental Medicine, Zurich, repeatedly obtained extracted teeth for a histopathological differential diagnosis between internal granuloma and invasive cervical resorption (ICR). Both constitute tooth resorptions, i. e. destructions of dental hard substances resulting from the activity of dentoclasts or osteoclasts. According to their starting point, tooth resorptions are classified as external and internal. External resorptions emanate from the periodontal root surface. They include surface, inflammatory, and (ankylosing) replacement resorptions as well as ICR.

Internal resorptions originate in the pulp cavity. The only representative is the internal granuloma (Tronstad 1988, Bakland 1992, Schroeder 1997, Gunraj 1999, Ne et al. 1999, Patel & Pitt Ford 2007).

With an estimated frequency of less than 0.1%, ICR is a relatively rare form of external resorption (Heithersay 1999b). It is distinguished by its localisation in the cervical root area, its invasive nature, and the formation of a mineralized substitution tissue resembling bone or cellular cementum, notably not associated with ankylosis (Heithersay 1999a). While the term "external granuloma" is widely used in German publications, various alternative expressions exist in the English literature: Odontoclastoma (Fish 1941), peripheral cervical resorption (Southam 1967), cervical external resorption (Makkes & Thoden Van Velzen 1975), (supraosseous) extracanal invasive resorption (Frank 1981, Frank & Bakland 1987), cervical or peripheral inflammatory root resorption (Tronstad 1988, Gold & Hasselgren 1992), subepithelial external root resorption (Trope 2002) or invasive cervical resorption (Heithersay 1999a).

The etiology and pathogenesis of ICR are largely obscure. A hypothesis regarding its development claims that a local discontinuity of the protecting layer of radicular cementum renders the subjacent dentin accessible for osteoclasts or dentoclasts (Hammarström & Lindskog 1992). In fact, voids in cementum frequently occur in the cervical root areas close to the cementoenamel junction (CEJ) (Schroeder & Scherle 1988, Neuvald & Consolaro 2000). These voids can arise as a primary malformation or secondarily result from a physical or chemical trauma. In agreement with this assumption, antecedent orthodontic treatment (24.1%), trauma (15.1%), or intracoronal bleaching (3.9%) have been found to be the most prevalent sole etiologic factors associated with ICR. However, about 16.4% of the lesions occurred without any apparent reason, i.e. were idiopathic (Heithersay 1999b).

There is wide consensus that ICR develops from the cervical periodontal tissues (Heithersay 2004). For unknown reasons, a well vascularized granulation tissue containing activated dentoclasts starts to invade the dentin and forms branched resorptive channels which encircle the pulp cavity, but do not penetrate across the innermost dentin. Wedenberg & Lindskog (1987) demonstrated that predentin contains a resorption inhibitor which prevents ICR from penetrating into the pulp cavity. As a result the resorption spreads in an apico-coronal direction and circumferentially along and around the root canal as soon as it reaches the predentin. While the lesion grows larger, a bone- or cementum-like hard tissue arises, which in part adheres to the resorbed dentin surfaces and in part forms fine trabeculae within the granulation tissue. In agreement with this pattern of progression, Heithersay (2004) distinguished four classes of ICR:

- Class I: small superficial resorptive lesion in the cervical root region;
- Class II: invasive resorptive lesion reaching close to the pulp cavity, but largely confined to coronal dentin;
- Class III: deep resorptive lesion penetrating also into the coronal third of the root;
- Class IV: large resorptive lesion extending below the coronal third of the root.

The diagnosis of ICR is challenging. Frequently it is detected incidentally in a routine intraoral radiograph, because lesions are usually painless and do not elicit any clinical signs (Heithersay 1999a). Resorption cavities located buccally or lingually often are not recognizable in conventional radiographs (Andreasen et al. 1987). Not surprisingly, therefore, a majority of lesions evaluated in a comprehensive survey (Heithersay 1999b) were already well advanced at the time of diagnosis. At this stage, they present an irregular radiolucency with indistinct margins and sometimes a mottled appearance. Under favorable conditions, the outline of the pulp chamber can be seen as a radiopaque line (Gold & Hasselgren 1992, Trope 1997, Frank & Torabinejad 1998, Heithersay 1999a, Patel et al. 2009). Particularly crucial is the differential diagnosis of ICR and internal granuloma, as ICR is often misdiagnosed as internal resorption. In Switzerland this is all the more critical, as according to paragraph 17a of the federal Krankenpflege-Leistungs-Verordnung (KLV), health insurances are held responsible for the therapy of so-called idiopathic internal granulomas, but do not have to pay for treatment of ICR, irrespective of whether or not it is idiopathic. The numerous requests regarding the distinction of ICR and internal granuloma show that their differential diagnosis apparently involves considerable uncertainties. The aim of our study was to evaluate, if and to what extent the size of the resorptive destruction, the formation of substitution tissue, and the pulp reaction associated with ICR have an impact on the radiographic visibility of diagnostic cardinal signs and, hence, account for these uncertainties.

Materials and Methods

Teeth Twelve permanent teeth extracted intact or in fragments which could be re-assembled were initially included in the evaluation. They were selected from a series of 22 specimens which had been sent between 2000 and 2008 to the Institute of Oral Biology, Section of Orofacial Development and Pathology, for a histopathologic differential diagnosis of internal granuloma and ICR. Upon microscopic examination, three of the twelve teeth were excluded, because one revealed a replacement resorption with ankylosis and two an inflammatory resorption. From the remaining nine specimens, intraoral radiographs were available; additional details are evident from Table I.

X-ray microtomographic (microCT) evaluation Five teeth were scanned in a µCT 20 microtomographic device (Scanco Medical, Brüttisellen, Switzerland) using a resolution of 1024×1024 px. Virtual slice thicknesses depended on the diameter of the examined teeth and ranged from 12 to 20 µm. Using the proprietary software of the microCT device, original images of the individual slices were converted into the RAW-format and imported in the 3D reconstruction program VGStudio Max (Volume Graphics, Heidelberg, Germany). Using this software, the radiographs were segmented manually, marking areas occupied by enamel and dentin, the pulp cavity, the resorptive defect and, if recognizable, mineralized substitution tissue. When particular segments were rendered transparent and suitable virtual sections were selected, the derived three-dimensional reconstructions allowed to visualize all components in their natural relationship.

Histologic processing All teeth were fixed either in 10% neutral formalin or a mixture of 4% paraformaldehyde and 0.2% glutaraldehyde in 0.1 M phosphate buffer (pH 7.2). After rinsing in 0.185 M Na-cacodylate buffer (pH 7.2), the fragments of fractured teeth were re-assembled with a commercial cyanoacrylate glue. Thereafter, all specimens were photographed using a M420 macroscope (Leica Microsystems, Heerbrugg, Switzerland) equipped with a DS-5M camera (Nikon, Egg, Switzerland) or a ProgRes C14+ camera (Jenoptik, Jena, Germany). Using a diamond band saw (EXAKT, Norderstedt, Germany) they were

Tab. I Clinical and light microscopic characteristics of the examined invasive cervical resorptions

	Gender[1]	Age[2]	Tooth	Stage[3]	Period. bone defect	Resorptive lesion					
						Connection to periodontium	Connection to pulp	Condition of pulp	Substitution tissue	Tertiary dentin	Resorption active
1	M	17-10	26	ES	no	yes	no	healthy	cellular	missing	no
2	M	16-9	36	ES	no	yes	no	healthy	cellular	missing	yes
3	M	42-3	11	AS	yes	yes	no	necrotic	acellular	cellular	no
4	F	50-9	35	AS	yes	yes	no	necrotic	cellular	cellular	no
5	M	74-6	35	AS	yes	yes	no	necrotic	cellular	cellular	no
6	F	22-7	35	LS	no	yes	yes	coronally pulpitic apically necrotic	cellular	missing	yes
7	F	65-9	13	LS	?	yes	no	necrotic	cellular	cellular	no
8	F	33-7	35	LS	?	yes	yes	necrotic	cellular	cellular	no
9	M	35-6	22	LS	yes	yes	yes	necrotic infected	cellular	cellular	no

[1] M = male, F = female
[2] in years-months
[3] ES = early stage, AS = advanced stage, LS = late stage

subsequently divided horizontally or along a bucco-lingual or mesio-distal plane parallel to the tooth axis. Part of these tissue blocks were decalcified in Morse's solution (49–50% formic acid, 10% Na-citrate) for about four weeks at room temperature and rinsed again in 0.185 M Na-cacodylate buffer. All specimens were dehydrated in ascending grades of ethanol. Thereafter decalcified tissue blocks were embedded in methyl-methacrylate (MMA; Sigma Aldrich, Buchs, Switzerland), undecalcified ones in Technovit 7200 VLC (Heraeus Kulzer, Wehrheim, Germany). From blocks embedded in MMA, sections of 5–7 µm in thickness were cut using a Reichert-Jung microtome 2050 Supercut (Leica Microsystems) and tungsten-carbide knives. They were deplasticized and stained with toluidine blue. Blocks embedded in Technovit were mounted on SEM aluminium stubs, polished with silicon carbide paper followed by diamond paste on a polishing cloth, and coated with a 10–15 nm thick layer of carbon. After examination in the scanning electron microscope (SEM), ground sections of about 50 µm in thickness were prepared using the EXAKT cutting-grinding system and stained with toluidine blue.

Microscopic evaluation A Tescan VEGA TS5316 XM (Tescan, Brno, Czech Republic) served for the SEM examination. In back-scattered electron mode, digital micrographs were captured using an accelerating voltage of 20 kV and a working distance of 23 mm. From the histologic sections, overview micrographs were made with the M420 macroscope, while a DM 6000B digital light microscope equipped with a DFC 420C camera (Leica Microsystems) was used for preparing the detail micrographs. The focus of the microscopic evaluation lay on the partition wall between the resorptive lesion and the pulp cavity, the amount and structure of the substitution tissue as well as on the appearance of the pulp and granulation tissue.

Results

Main clinical and light microscopic characteristics of the ICR lesions examined are summarized in Table I. Extracted teeth were obtained from four female and five male patients ranging in age from 16-9 to 74-6 (years-months). Intraoral radiographs from four of the nine teeth revealed a periodontal bone defect, in two specimens periodontal conditions could not be judged unambiguously. Histologically, a connection between the ICR and the periodontium was evident in all of the nine teeth, while in two a connection existed with the pulp. Irrespectively, the pulp was perfectly healthy in only two cases, while in the remaining specimens it was inflamed or necrotic. In six instances the pulp had formed tertiary dentin as a reaction on the resorption. Bone- or cementum-like substitution tissue could be found in all resorptive lesions, but only in two of them the resorption was ongoing at the time of extraction, i. e. there were multinucleated giant cells along the margins of the resorptive cavities.

A preliminary overview over the histologic findings suggested that depending on the size of the resorptive defects, the ICR lesions could be assigned to three stages. Two lesions were classified as early, three as advanced, and four as late stages (Tab. I). The detailed findings are presented separately for these subgroups.

Early stage (Fig. 1, 2) In intraoral radiographs, the resorptive defect presented a relatively inhomogeneous (Fig. 1a) or rather homogeneous (Fig. 2b) radiolucency with indistinct margins and an irregular contour, which revealed a connection with the periodontal space only under favorable conditions of projection (Fig. 1a). Sometimes the radiolucency was superimposed on the pulp cavity, and a partition wall between root canal and resorptive lesion was not visible (Fig. 2b). The alveolar bone was always inconspicuous.

Macroscopically the color of the crowns appeared normal, and local portals of the ICR lesions towards the periodontium in the area of the CEJ could be surmised (Fig.1b, 2d). MicroCT reconstructions (Fig. 1c–e, 2c, e, f) demonstrated that the resorptive lesions had already partly encircled the pulp cavity. However, the root canals were separated from the resorptive defects by a continuous, thick layer of dentin. Connections with the periodontal space were generally small and sometimes multiple. Mineralized substitution tissue exhibited a radioden-

sity similar to that of dentin and could be unambiguously identified only when it was surrounded by uncalcified material.

Histologically the substitution tissue could be clearly identified. It occurred both along the resorbed dentin margins and scattered within the granulation tissue, appearing as cellular material resembling bone or cementum (Fig. 1g, 2k). Resorbed dentin revealed characteristically scalloped margins which foreshadow antecedent Howship's lacunae. However, multinucleated giant cells, i. e. dentoclasts, in contact to dentin could be found only occasionally (Fig. 2i). Granulation tissue occupying interstitial spaces sometimes contained sparse inflammatory cells (Fig. 2i). The dentinal partition wall between the resorptive defect and the root canals, including layers of odontoblasts and predentin, was continuously intact (Fig. 1g, 2k). Correspondingly, no signs of inflammation were observed in the pulp.

Advanced stage (Fig. 3) In intraoral radiographs, advanced lesions presented mostly inhomogeneous, sometimes mottled radiolucencies with indistinct margins (Fig. 3a, m), which clearly communicated with the periodontal space. However, there were also lesions which appeared relatively homogeneous and radiodense and, hence, were poorly visible (Fig. 3h). Resorptive defects were often projected on the root canals which were sometimes obliterated. A partition wall between the pulp cavity and the radiolucency was only partly visible. In all instances there was a periodontal bone defect where the lesion penetrated across the root surface.

Macroscopically the connection to the periodontium was from about 2 mm (Fig. 3b, j) to 5 mm (Fig. 3o) in diameter. A microCT reconstruction existed only from one specimen. It showed that the resorptive defect did not communicate with the pulp and the partition wall consisting of tertiary dentin was continuous. Mineralized substitution tissue, if present, could not be distinguished from dentin. However, it clearly stood out against the radicular dentin in the SEM, appearing as a cellular mineralized tissue (Fig. 3l, p).

Histologically resorptive defects contained variable amounts of granulation tissue (Fig. 3e) with inflammatory cell infiltrates and, in one instance, microbial plaque (Fig. 3f). In none of the ICR lesions at the advanced stage were there multinucleated giant cells. Cellular mineralized substitution tissue almost completely filled part of the resorptive defects (Fig. 3l), while in others, it occupied only small areas on the resorbed dentinal margins (Fig. 3p). A noticeable feature in one instance was a thin layer of cell-free substitution tissue in the periphery of the radicular dentin (Fig. 3g). A communication between the resorptive lesion and the pulp did not exist in any of the teeth. However, a pulp reaction in the form of tertiary dentin could usually be observed. In part, this tertiary dentin contained cells and considerably narrowed the pulp cavity (Fig. 3f, l).

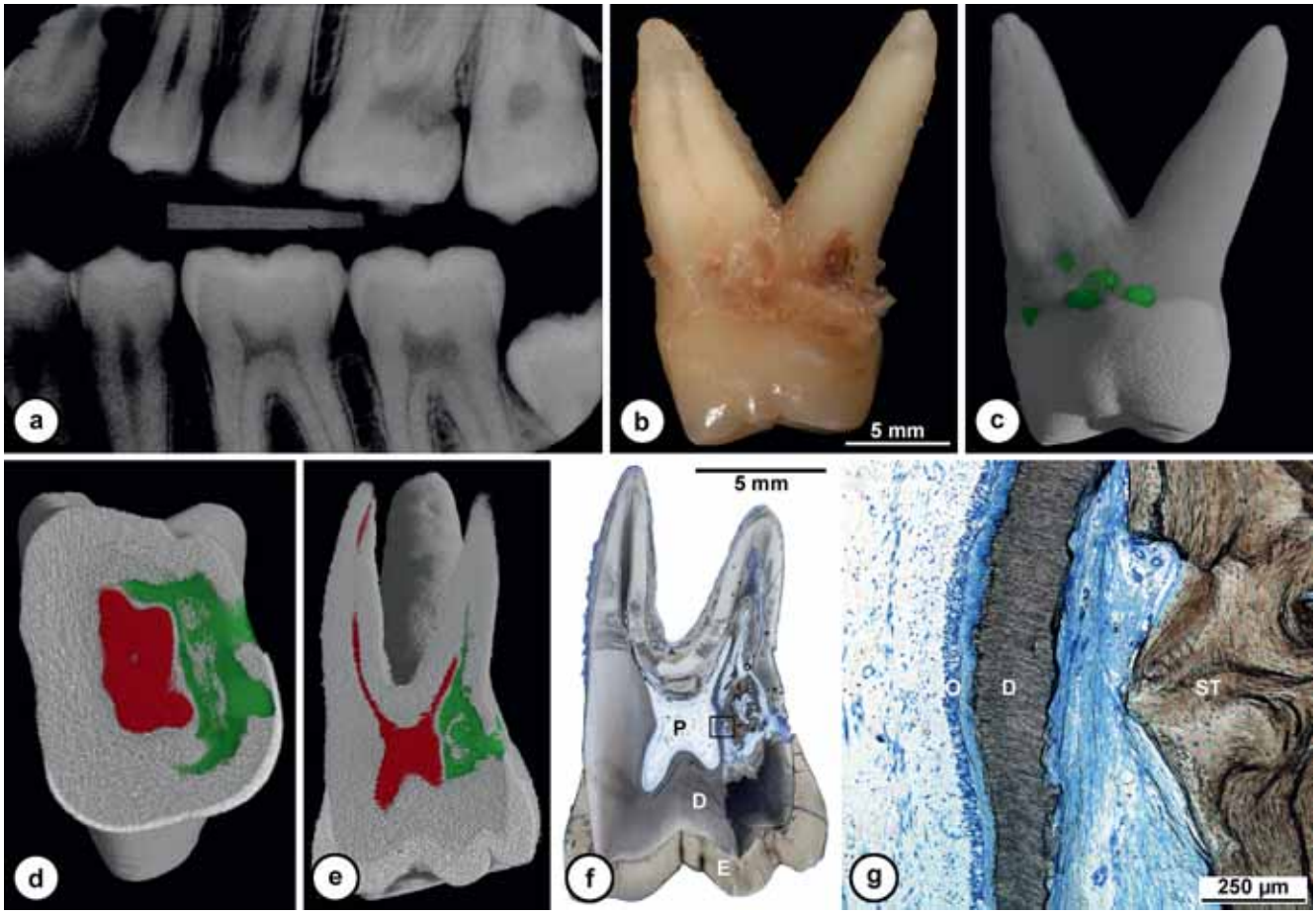

Fig. 1 Early stage of slowly progressive ICR. a: Intraoral radiograph at the age of 16 years. b, c: Distal views of tooth 26 (b) and the corresponding microCT reconstruction (c; in green = connections of the resorptive defect to the periodontium). d, e: Horizontal section approximately at the cemento-enamel junction (d) and mesio-distal section across the buccal roots (e) in the microCT reconstruction; note the continuous separation of the resorptive defect (in green) and the pulp cavity (in red). f: Overview micrograph of a ground section corresponding approximately to the virtual section e; the rectangle marks the location of detail g. g: Detail micrograph of the boundary region between the pulp and resorptive cavity; note the intact seams of predentin and odontoblasts (O). E = enamel, D = dentin, P = pulp, ST = substitution tissue. Original magnifications b, f: 1.3×; g: 50×.

Late stage (Fig. 4) In one late case, the rapid progression of the external resorption was documented radiographically. A first intraoral X-ray at the age of 22-2 revealed a radiolucency with a blurred margin (Fig. 4a), 5 months later, the lesion presented a well-defined ellipsoid image, similar to an internal granuloma (Fig. 4b). Although the radiolucency was projected onto the pulp cavity a partition wall was visible between the root canal and the resorption cavity. However, no clear connection with the periodontal space could be recognized and the alveolar bone appeared inconspicuous (Fig. 4b).

Teeth with ICR at the late stage always exhibited a macroscopically visible, extensive connection of the resorption cavity with the periodontium (Fig. 4d, e). The microCT reconstruction revealed a seemingly intact partition wall against the root canal, while substitution tissue could not be recognized (Fig. 4c, f). In contrast to the microCT reconstruction the examination with the SEM showed that the dentinal wall around the coronal por-

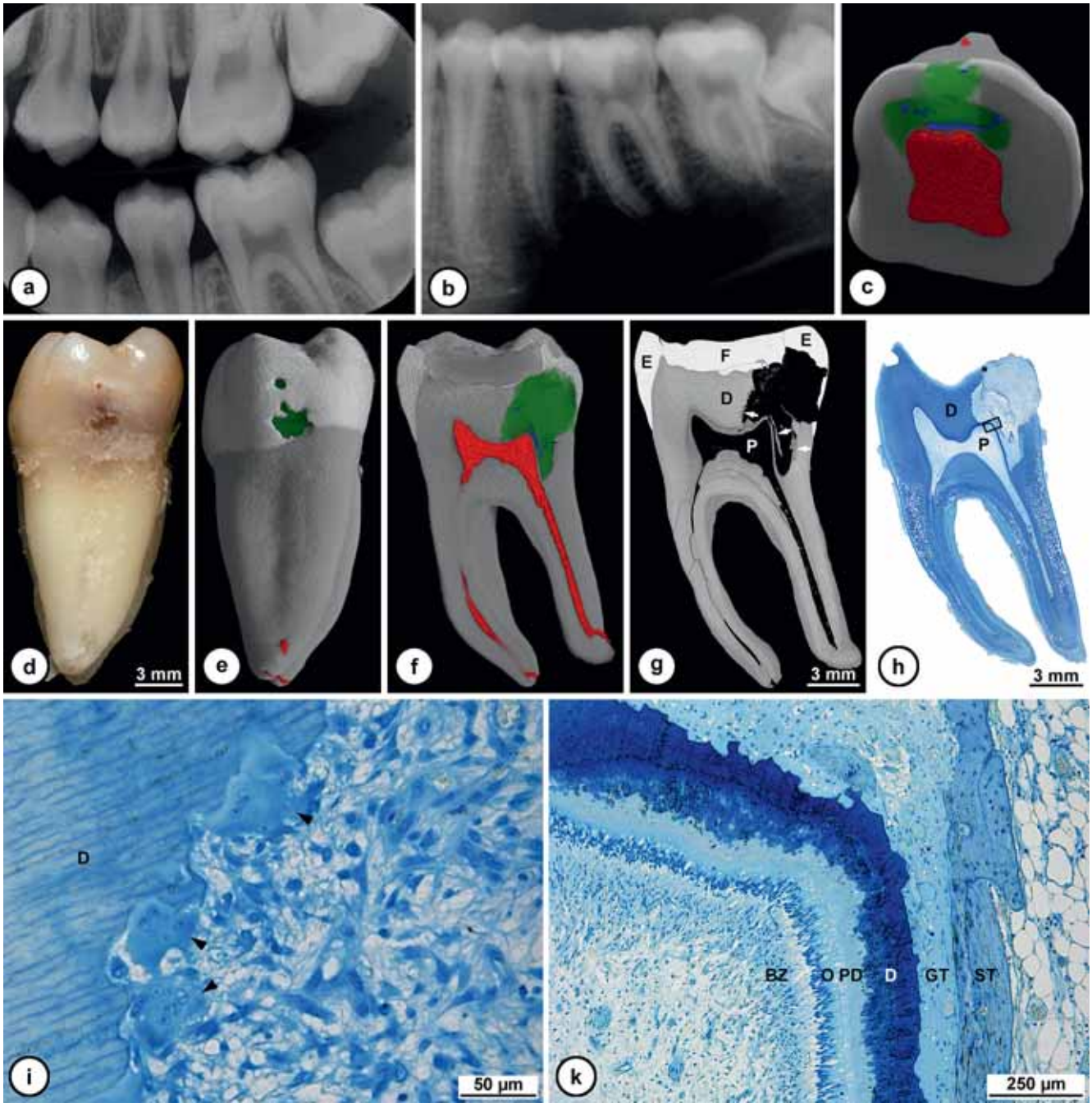

Fig. 2 Early stage of rapidly progressive ICR. a, b: Intraoral radiographs at the ages of 11-11 (years-months; a) and 16-3 (b). c, f: Horizontal section across the cervical region (c) and axial mesio-distal section (f) in the microCT reconstruction (in green = resorptive defect, in red = pulp cavity, in blue = substitution tissue). d, e: Distal views of tooth 36 (d) and the microCT reconstruction (e; in green = connections of the resorptive defect with the periodontium). g, h: Overview micrographs of a ground section corresponding approximately to the virtual section f imaged using SEM backscattered electron mode (g) and of a histologic section viewed with bright field illumination (h); arrows in g point at substitution tissue, the tiny rectangle (close to the upper margin) and the large rectangle in h mark the location of the details i and k. i, k: Details of the border between dentin and resorptive defect (i) as well as of the pulpal wall in the region of the resorption (k); arrow-heads in i indicate dentoclasts; note the intact layers of odontoblasts (O) and predentin (PD). BZ = bipolar zone, D = dentin, E = enamel, F = filling, GT = granulation tissue, P = pulp, ST = substitution tissue. Original magnifications d, h: 1.3×; g: 40×; i: 200×; k: 50×.

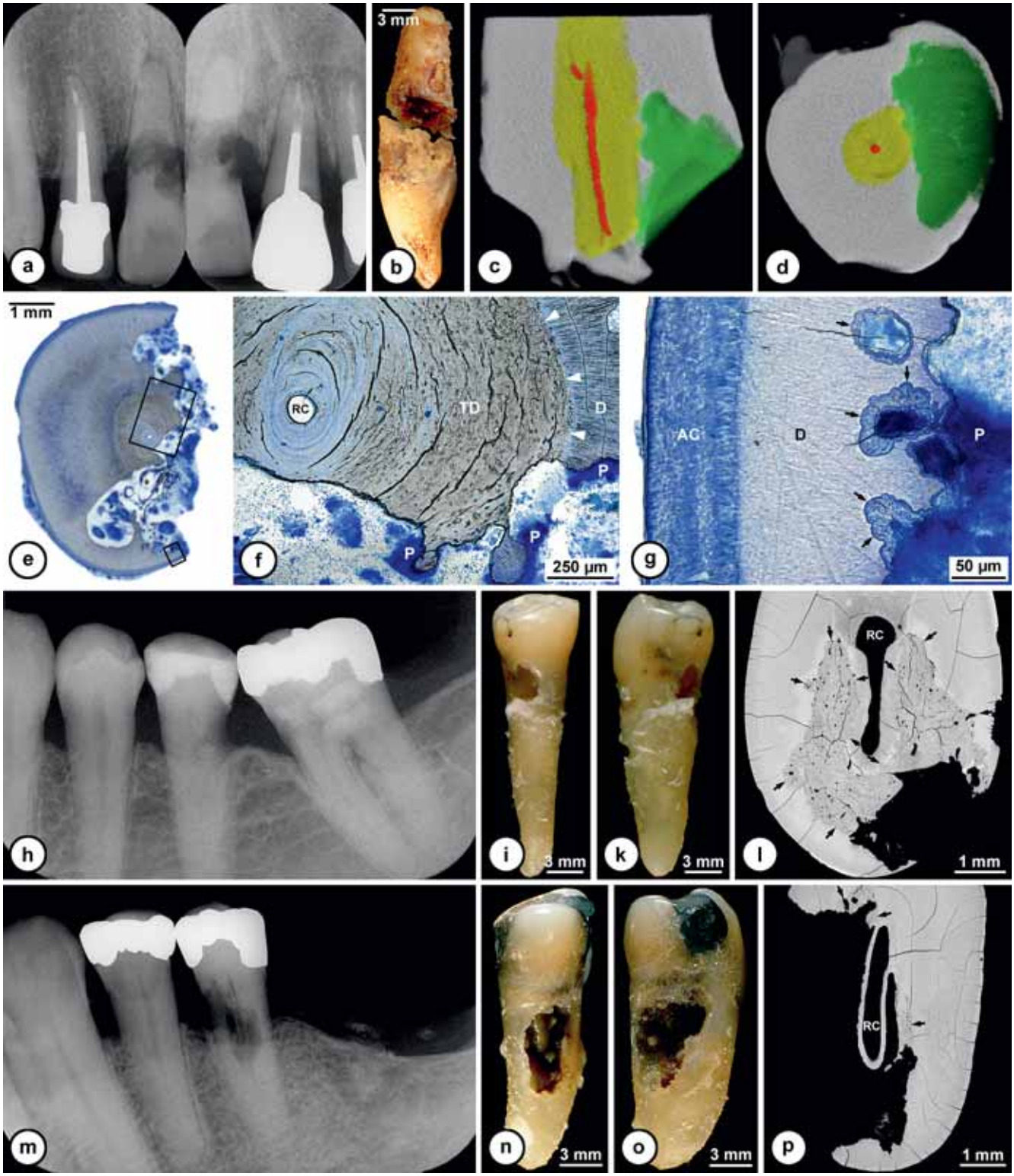

Fig. 3 Advanced stages of ICR characterized by extensive deposition of tertiary dentin (a–g) as well as by prominent (h–l) and sparse (m–p) formation of substitution tissue. a–g: Intraoral radiograph at the age of 42-3 (a); mesial view of the fragmented tooth 11 (b); labio-lingual (c) and horizontal (d) sections across the coronal part of the root fragment in the microCT reconstruction (in green = resorptive defect, in red = root canal, in yellow = tertiary dentin); overview (e) and detail (f, g) micrographs of a ground section corresponding approximately to the virtual section d; the rectangles in e mark the locations of the details f and g; note in f the thick layer of cellular tertiary dentin (TD) and its completely smooth border (arrow-heads) against regular radicular dentin (D); in contrast, sparse cementum-like substitution tissue (g) is restricted to scalloped dentin margins (arrows) in the periphery of the root. AC = acellular extrinsic fiber cementum, P = plaque. h-p: Intraoral radiographs at ages of 51-10 (h) and 74-1 (m); lingual (i, n) and approximal (k, o) views of two teeth 35; micrographs of two horizontal ground sections imaged using SEM backscattered electron mode (l, p); note the different amounts of cellular substitution tissue (arrows) which in both cases is completely separated from the root canals (RC) by a layer of dentin. Original magnifications b: 1.1×; e, l, k: 1.3×; f: 50×; g: 200×; l, p: 80×; n, o: 1.6×.

tion of the pulp was not continuously intact. Moreover, there were small islands of mineralized substitution tissue (Fig. 4h).

Histologically, the granulation tissue of late stage lesions also contained inflammatory cell infiltrates as well as cellular substitution tissue (Fig. 4k). Occasionally Howship's lacunae revealing multinucleated giant cells (dentoclasts) were observed (Fig. 4i). The dentinal wall between the root canal and the resorptive defect was partially fenestrated and partially dissolved. In fenestrated areas, layers of predentin and odontoblasts were sometimes still present, but sometimes had disappeared when the adjacent pulp tissue contained an inflammatory cell infiltrate (Fig. 4k). Where a dentinal wall was missing, the pulp was necrotic.

Discussion

The findings of this study show that irrespective of the size of ICR lesions, distinct patterns exist with respect to resorptive activity and formation of mineralized substitution tissue, which significantly affect the radiographic diagnosis.

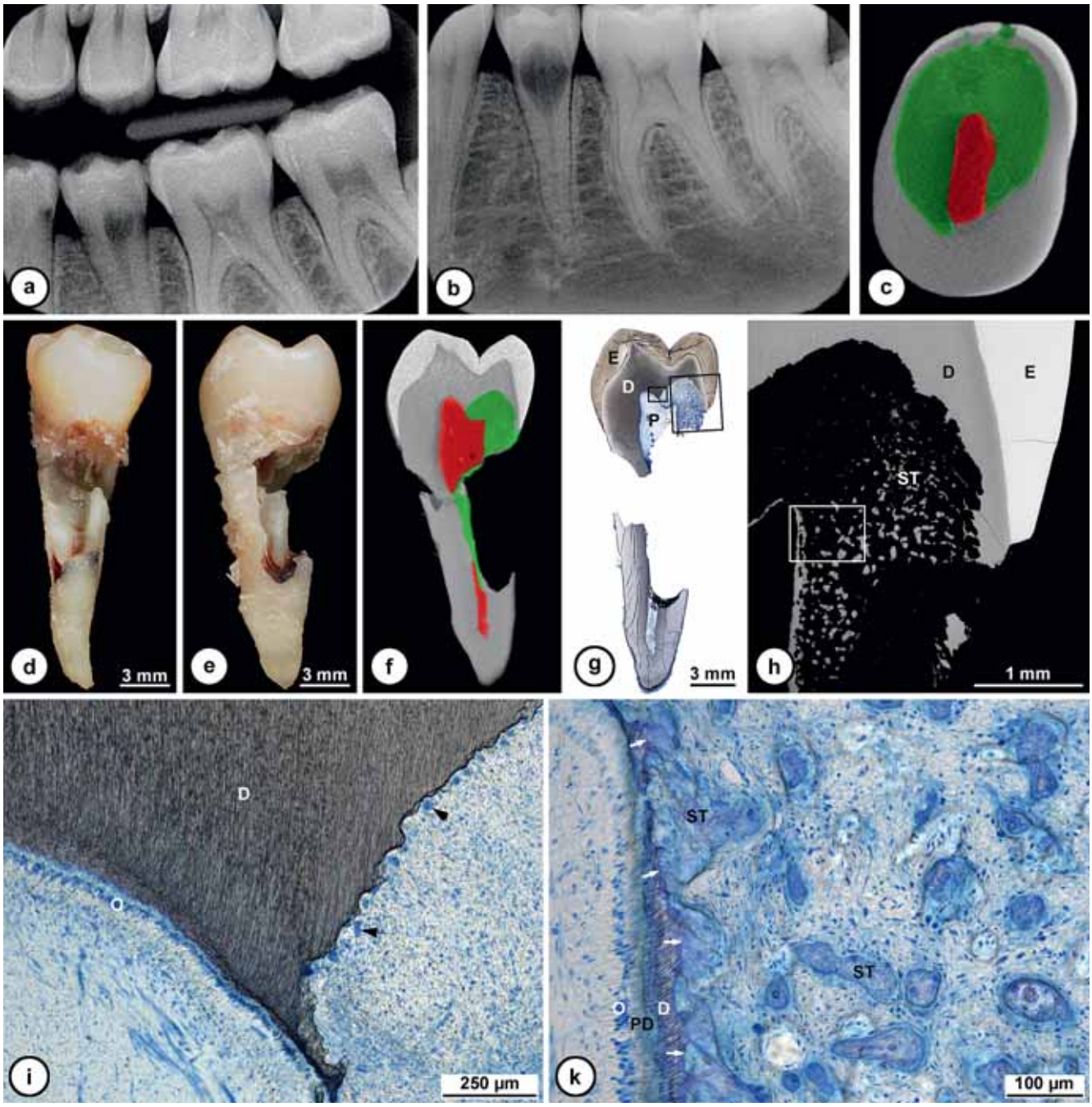

Fig. 4 Late stage of progressive ICR. Intraoral radiographs at the age of 22-2 (a) and 22-7 (b); note in b the clearly visible wall of the root canal within the ellipsoid radiolucency; horizontal section across the cervical region (c) and bucco-lingual section (f) in the microCT reconstruction (in green = resorptive defect, in red = pulp cavity); lingual (d) and distal (e) views of tooth 35; overview (g) and detail (h–k) micrographs of a ground section corresponding approximately to the virtual section f imaged using SEM backscattered electron mode (h) and viewed in bright field illumination (i, k); the rectangles in g mark the locations of the details h and i, the rectangle in h indicates the approximate location of the detail k; note the dentoclasts along the dentin (arrow-heads in i) and the delicate trabecular substitution tissue (ST) deposited on a thin dentinal wall (D) around the pulp (arrows in k). D = dentin, E = enamel, O = odontoblasts, P = pulp, PD = predentin. Original magnifications d, e, g: 1.3×; h: 150×; i: 50×; k: 100×.

A problem of the present study is the limited number of finally usable cases. The reason for the eliminations were always multiple fractures of the teeth upon extraction, which prevented a reconstruction of the real topographical relationship between the resorptive lesion and the pulp cavity. As a consequence of the small sample size, no statistical correlations could be made between the histological and radiographic findings. Also due to the small sample size, the examined lesions were classified into three stages, whereas Heithersay (2004) in regard to the therapy distinguished four classes. The restriction to three stages seemed to make all the more sense, as the classes II and III defined by Heithersay are difficult to distinguish histologically. They approximately correspond to the advanced stage identified in this investigation, while the classes I and IV more or less coincide with the early and late stages, respectively.

The following discussion of our own findings takes into consideration established diagnostic criteria concerning the identification of ICR and its distinction from internal granuloma. A pink discoloration ("pink spot") in the cervical crown region is frequently listed as a clinical sign of ICR (Trope 1997, Heithersay 1999a, Patel et al. 2009). However, none of the specimens examined revealed a discoloration. This could be due to the missing blood supply of granulation tissue in extracted teeth, which consequently would shine less through even thin dentin. Irrespectively, a pink discoloration cannot be taken as an indication of ICR, because it may as well result from an internal granuloma (Mummery 1920, Bakland 1992, Gunraj 1999, Ne et al. 1999, Patel & Pitt Ford 2007, Patel et al. 2010).

Several authors (Gold & Hasselgren 1992, Trope 1997, Patel et al. 2009) mention as a further clinical sign of ICR that periodontal probing causes profuse bleeding because the resorptive granulation tissue located in the cervical area is well vascularized. In fact it is commonly assumed that ICR develops from chronically inflamed tissue in the vicinity of a periodontal pocket. However, in agreement with previous findings (Heithersay 1999a), a radiographic periodontal defect was observed only in association with advanced stage lesions, and even a tooth with ICR at the late stage presented inconspicuous periodontal conditions. This raises the question, whether a periodontal break-down indeed constitutes a consequence, rather than the cause of a long persisting inflammatory root resorption.

Two radiographic features are considered as signs of ICR: (1) a communication of the resorptive defect with the periodontal space and (2) an intact dentinal wall against the pulp cavity (Gold & Hasselgren 1992, Trope 1997, Frank & Torabinejad 1998, Heithersay 1999a, Patel et al. 2009). Although histologically all examined specimens showed a connection of the resorptive lesion with the periodontium, it often was not evident in intraoral radiographs particularly at early stages. An explanation was provided by the microCT evaluation which revealed that the periodontal portals of early lesions were generally too small to be identifiable radiographically, even when they were located approximally. Just as difficult to recognize was the dentinal wall between the resorptive defect and the pulp cavity even when it was relatively thick and completely intact histologically. In contrast to conventional radiographs microCT reconstructions clearly disclosed this feature as well.

The microscopic evaluation revealed that in all resorptive cavities, cellular mineralized substitution tissue had been formed, although in varying amounts. In the microCT reconstructions, this hard tissue could only be identified, when it was surrounded by unmineralized material. If it had been deposited on the resorbed dentinal margins, it could not be distinguished from dentin, because it exhibited a similar radiodensity. The contents of substitution tissue in the resorptive lesion affected the radiographic visibility of ICR. Lesions containing large amounts of bone-like material were difficult to recognize in the radiographs and, therefore, could easily be overseen.

In regard to the treatment of ICR, a reliable estimate of its extension is essential. Heithersay (2004) recommended to conservatively treat only class I, II, and III lesions and to extract teeth with class IV defects. The challenge is to judge the true extension, which is impossible using conventional radiographic techniques, particularly when lesions are located buccally or lingually. If it is additionally taken into account that the cardinal signs of ICR are often difficult or impossible to recognize in conventional radiographs, three-dimensional imaging, for example using cone beam computed tomography (CBCT) seems warranted if an internal or external root resorption is suspected (Bergmans et al. 2002, Patel & Dawood 2007, Patel et al. 2009). Although microCT reconstructions, depending on the size of the tooth examined, yield a voxel size of about 16–32 µm, the resolution of 70–80 µm obtained with modern CBCT devices would appear sufficient to identify the essential features of ICR, if an appropriate field of view is selected. In fact, a recent *ex vivo* investigation (Kamburoğlu et al. 2011) indicated that a CBCT image is significantly superior to a conventional radiograph concerning the identification and localization of a resorptive defect.

Acknowledgments

The authors are grateful to Jacqueline Hofmann-Lobsiger and Jinan Fierz for skillful preparation of the microscopic slides. Thanks are also due to the Clinic of Preventive Dentistry, Periodontology and Cariology (Dr. Frank Paqué) for making available the microCT device. Last but not least we thank the referring colleagues for providing the intraoral radiographs.

Résumé

Le but de cette étude était d'évaluer si la structure histologique des résorptions cervicales invasives (granulomes externes) affecte leur diagnostic radiographique clinique et comment. Pour ce faire, neuf dents extraites, plus ou moins intactes, dont les radiographies intra-orales étaient disponibles, ont été examinées au microscope électronique à balayage (MEB) ainsi qu'en microscopie optique. Pour certains spécimens, des coupes non décalcifiées furent préparées, alors que d'autres furent décalcifiées pour la préparation de coupes histologiques. Cinq dents furent scannées par un microtomographe à rayons X (microCT) et reconstruites digitalement en trois dimensions.

Trois caractéristiques histologiques: (1) la localisation et l'extension du défaut résorptif, (2) la taille de la communication avec le parodonte et (3) la quantité de tissus de substitution minéralisés formée dans la lésion ont affecté le diagnostic radiographique. A des stades précoces et avancés, les résorptions cervicales invasives avaient encerclé les cavités pulpaires, toutefois sans détruire la dentine profonde. Même si le mur dentinaire adjacent à la pulpe était histologiquement intact et épais, cette importante caractéristique diagnostique n'a fréquemment pas pu être identifiée à partir de radiographies conventionnelles. De plus, la communication entre la lésion résorptive et le parodonte était souvent invisible en radiogra-

phie, bien qu'elle ait toujours pu être identifiée au cours des évaluations microscopiques, particulièrement à des stades précoces lorsqu'elle est très petite. Les résorptions cervicales invasives contenant de grandes quantités de tissus de substitution minéralisés furent difficiles à identifier, et par conséquent, purent facilement être manquées.

Ainsi, trois caractéristiques considérées comme essentielles pour le diagnostic différentiel des résorptions cervicales invasives n'ont pas été observées sur des radiographies conventionnelles. Parmi ces trois caractéristiques, le mur dentinaire contre la cavité pulpaire et la communication vers le parodonte ont été, cependant, clairement visibles sur les reconstructions du microCT.

References

Andreasen F M, Sewerin I, Mandel U, Andreasen J O: Radiographic assessment of simulated root resorption cavities. Endod Dent Traumatol 3: 21–27 (1987)

Bakland L K: Root resorption. Dent Clin North Am 36: 491–507 (1992)

Bergmans L, Van Cleynenbreugel J, Verbeken E, Wevers M, Van Meerbeek B, Lambrechts P: Cervical external root resorption in vital teeth. X-ray microfocus-tomographical and histopathological case study. J Clin Periodontol 29: 580–585 (2002)

Fish E W: Benign neoplasia of tooth and bone. Proc R Soc Med 34: 427–446 (1941)

Frank A L: External-internal progressive resorption and its nonsurgical correction. J Endod 7: 473–476 (1981)

Frank A L, Bakland L K: Nonendodontic therapy for supraosseous extracanal invasive resorption. J Endod 13: 348–355 (1987)

Frank A L, Torabinejad M: Diagnosis and treatment of extracanal invasive resorption. J Endod 24: 500–504 (1998)

Gold S I, Hasselgren G: Peripheral inflammatory root resorption. A review of the literature with case reports. J Clin Periodontol 19: 523–534 (1992)

Gunraj M N: Dental root resorption. Oral Surg Oral Med Oral Pathol Oral Radiol Endod 88: 647–653 (1999)

Hammarström L, Lindskog S: Factors regulating and modifying dental root resorption. Proc Finn Dent Soc 88 Suppl 1: 115–123 (1992)

Heithersay G S: Clinical, radiologic, and histopathologic features of invasive cervical resorption. Quintessence Int 30: 27–37 (1999a)

Heithersay G S: Invasive cervical resorption: An analysis of potential predisposing factors. Quintessence Int 30: 83–95 (1999b)

Heithersay G S: Invasive cervical resorption. Endod Topics 7: 73–92 (2004)

Kamburoğlu K, Kurşun Ş, Yüksel S, Öztaş B: Observer ability to detect *ex vivo* simulated internal or external cervical root resorption. J Endod 37: 168–175 (2011)

Makkes P C, Thoden Van Velzen S K: Cervical external root resorption. J Dent 3: 217–222 (1975)

Mummery J H: The pathology of "pink spots" on teeth. Br Dent J 41: 301–311 (1920)

Ne R F, Witherspoon D E, Gutmann J L: Tooth resorption. Quintessence Int 30: 9–25 (1999)

Neuvald L, Consolaro A: Cementoenamel junction: Microscopic analysis and external cervical resorption. J Endod 26: 503–508 (2000)

Patel S, Dawood A: The use of cone beam computed tomography in the management of external cervical resorption lesions. Int Endod J 40: 730–737 (2007)

Patel S, Kanagasingam S, Pitt Ford T: External cervical resorption: A review. J Endod 35: 616–625 (2009)

Patel S, Pitt Ford T: Is the resorption external or internal? Dent Update 34: 218–229 (2007)

Patel S, Ricucci D, Durak C, Tay F: Internal root resorption: A review. J Endod 36: 1107–1121 (2010)

Schroeder H E: Pathobiologie oraler Strukturen. Zähne, Pulpa, Parodont. 3. Aufl., Karger, Basel (1997)

Schroeder H E, Scherle W F: Cemento-enamel junction – revisited. J Periodontal Res 23: 53–59 (1988)

Southam J C: Clinical and histological aspects of peripheral cervical resorption. J Periodontol 38: 534–538 (1967)

Tronstad L: Root resorption – etiology, terminology and clinical manifestations. Endod Dent Traumatol 4: 241–252 (1988)

Trope M: Cervical root resorption. J Am Dent Assoc 128 Suppl: 56S–59S (1997)

Trope M: Root resorption due to dental trauma. Endodontic Topics 1: 79–100 (2002)

Wedenberg C, Lindskog S: Evidence for a resorption inhibitor in dentin. Scand J Dent Res 95: 205–211 (1987)